

Multifractality of Hamiltonians with power-law transfer terms

E. Cuevas*

Departamento de Física, Universidad de Murcia, E-30071 Murcia, Spain.

(Dated: January 29, 2020)

Finite size effects in the generalized fractal dimensions d_q are investigated numerically. We concentrate on a one-dimensional disordered model with long-range random hopping amplitudes in both the strong and the weak coupling regime. At the macroscopic limit, a linear dependence of d_q on q is found in both regimes for values of $q \lesssim 4g^{-1}$, where g is the coupling constant of the model.

PACS numbers: 71.30.+h, 72.15.Rn, 73.20.Jc, 05.45.Df

I. INTRODUCTION

Quantum phase transitions in disordered electronic systems remain one of the central problems in condensed matter physics. Considerable attention has recently focused on the critical eigenfunctions, which strongly fluctuate near the critical point and thus have multifractal scaling properties^{1,2,3,4,5}. Wavefunction statistics can be characterized through the set of generalized fractal dimensions d_q which are associated to the scaling of the q th moment of the wavefunction intensity. A complete knowledge of d_q is equivalent to a complete physical characterization of the fractal¹.

Metal insulator transitions (MITs) depend on the dimensionality and symmetries of the system and can occur in both the strong disorder and the weak disorder regime (strong coupling or weak coupling regime, respectively, of the corresponding field-theoretical description). Each regime is characterized by its respective coupling strength g , which depends on the ratio between diagonal disorder and the off-diagonal transition matrix elements of the Hamiltonian⁶.

For a multifractal structure of wavefunctions, the q -dependence of the fractal dimensions d_q is given by the linear relation

$$d_q = d - c_g q, \quad c_g \ll 1, \quad (1)$$

where c_g is a small parameter related to the coupling constant of the corresponding model. This equation has been obtained for different transitions in the weak coupling limit using different approaches, which we summarize in the next paragraphs. Eq. (1) describes *weak multifractality* in the sense that the fractal dimensions d_q slightly deviate from the system dimensionality d characteristic of the homogeneously spread metallic wavefunctions.

In the context of the theory of Anderson localization, Eq. (1) was obtained³, in the leading order in $1/2\pi\nu D \ll 1$, for 2D conductors on the basis of a reduced version of the supersymmetric σ -model. In this case $c_g = 1/2\pi^2\nu\beta D$, where ν is the density of states, D the diffusion constant and β the symmetry parameter.

Using a perturbative ϵ -expansion in one-loop order for a $d = 2 + \epsilon$ dimensional system, Eq. (1) was found⁷, in the leading order in $\epsilon \ll 1$, with $c_g = \epsilon$. This derivation was made for the case of unbroken time-reversal symmetry

(orthogonal universality class) in the weak coupling limit.

Ref.⁸ derived Eq. (1) with $c_g = g/8\pi$, in the limit $g \ll 1$ for the power-law random matrix model (orthogonal universality class). This solution was found by mapping the problem onto a nonlinear σ -model with nonlocal interaction.

Eq. (1) was also obtained, using the replica trick⁹, for the critical wavefunction of a 2D Dirac fermion in a random vector potential (chiral universality class). The $c_g = \Delta_A/\pi$ found depends on the variance Δ_A of the Gaussian distributed vector potential. This result was confirmed recently^{10,11} by mapping the problem to a Gaussian field theory in an ultrametric space.

Field-theoretical approaches in the context of the integer quantum Hall transition (unitary universality class) have been addressed recently. Based on the application of conformal field theory to the critical point of a 2D Euclidean field theory, Bhasen *et al.*¹² derived Eq. (1) with $c_g = 2/k$, where k is the inverse coupling constant.

However, we wish to point out that there are several reasons why the existing theories remain unsatisfactory. Most importantly, MITs generically take place at strong disorder, where the energy scales associated with both disorder and interactions are comparable to the Fermi energy, unlike to what happens in perturbative $2 + \epsilon$ expansion approaches or in effective field theories. Thus, quantitative results for d_q are lacking at strong coupling, and finding d_q for this regime is essential in order to fully understand the MITs.

The aim of this work was twofold. First, a numerical verification of the weak coupling phase result, Eq. (1). Second, and most importantly, we were interested in finding the q -dependence of d_q in the strong coupling regime, which has been left unexplored. Since this case is not accessible by the previous treatments, the problem can only be addressed by using numerical calculations.

The paper begins by first giving the model and the methods used for the calculations in Sec. II. The results for the fractal dimensions in the weak and the strong coupling regimes are presented in Subsec. III A and III B, respectively. Finally, Sec. IV summarizes our findings.

II. MODEL AND METHODS

The disorder-induced MIT is usually investigated for Hamiltonians with short-range, off-diagonal matrix elements (*e.g.*, the canonical Anderson model). Other Hamiltonians exhibiting an MIT in arbitrary dimension d are those that include long-range hopping terms^{13,14}. The effect of long-range hopping on localization was originally considered by Anderson¹⁵ for randomly distributed impurities in d dimensions with the $V(\mathbf{r}-\mathbf{r}') \sim |\mathbf{r}-\mathbf{r}'|^{-\alpha}$ hopping interaction. It is known^{15,16} that all states are extended for $\alpha < d$, whereas for $\alpha > d$ the states are localized. Thus, the MIT can be studied by varying the exponent α at fixed disorder strength. At the transition line $\alpha = d$, a real space renormalization group can be constructed for the distribution of couplings^{16,17}. These models are the most convenient for studying critical properties numerically since the exact quantum critical point is known ($\alpha = d$) and, in addition, they allow the 1D case to be treated, thus using larger system sizes and reducing the numerical effort. Many real systems of interest can be described by these Hamiltonians. Among such systems are optical phonons in disordered dielectric materials coupled by electric dipole forces, excitations in two-level systems in glasses interacting via elastic strain, magnetic impurities in metals coupled by an r^{-3} RKKY interaction and impurity quasi-particle states in 2D disordered d -wave superconductors.

We will consider here the intensively studied power-law random banded matrix model (PRBM)^{4,5,8,18,19,20,21,22,23}. The corresponding Hamiltonian, which describes a disordered 1D sample with random long-range hopping, is represented by real symmetric matrices, whose entries are randomly drawn from a normal distribution with zero mean, $\langle \mathcal{H}_{ij} \rangle = 0$, and a variance which depends on the distance between lattice sites

$$\langle |\mathcal{H}_{ij}|^2 \rangle = \frac{1}{1 + (|i-j|/b)^2} \times \begin{cases} \frac{1}{2}, & i \neq j \\ 1, & i = j \end{cases}, \quad (2)$$

where the parameter b plays the role of the inverse coupling constant $b = 4g^{-1}$ of the corresponding σ -model at the center of the spectral band. The model describes a whole family of critical theories parametrized by $0 < b < \infty$, which determines the critical dimensionless conductance, in the same way as the dimensionality labels the different Anderson transitions. In the two limiting cases, $b \gg 1$ and $b \ll 1$, which correspond to the weak and the strong disorder limits, respectively, some critical properties have been derived analytically^{4,8,18,22,23}. More specifically, as already mentioned in the Introduction, Ref.⁸ derived the following equation in the limit $b \gg 1$

$$d_q = 1 - \frac{q}{2\pi b}, \quad q \ll 2\pi b. \quad (3)$$

The system size ranges between $L = 180$ and $L = 5400$, and $0.01 \leq b \leq 12$. We restrict ourselves to values of

$q \lesssim b$, and consider a small energy window, containing about 5% of the states around the center of the band. The number of random realizations is such that the number of critical states included for each L is roughly 4×10^5 , while, in order to reduce edge effects, periodic boundary conditions are included. Using methods based on level statistics, we checked that the normalized nearest level variances²⁴ are indeed scale-invariant at each critical point studied.

For the computation of d_q we used the standard box-counting procedure², first dividing the system of L sites into $N_l = L/l$ boxes of linear size l and determining the box probability of the wavefunction in the i box by $p_i(l) = \sum_n |\psi_{kn}|^2$, where the summation is restricted to sites within that box, and ψ_{kn} denotes the amplitude of an eigenstate with energy E_k at site n . The normalized q th-moments of this probability constitute a measure. From this, the mass exponents, $\tau_q(L)$, which encode generalized dimensions $d_q(L) = \tau_q(L)/(q-1)$, can be obtained²⁵

$$\tau_q(L) = \lim_{\delta \rightarrow 0} \frac{\ln \sum_{i=1}^{N_l} p_i^q(l)}{\ln \delta}, \quad (4)$$

where $\delta = l/L$ denotes the ratio of the box sizes and the system size. It should be made clear that the calculation of $\tau_q(L)$ is suitable only if the conditions²

$$a \ll l < L \ll \xi, \quad (5)$$

are satisfied, where ξ is the localization or correlation length and a is the lattice spacing (or any microscopic length scale of the system). In practice, $\tau_q(L)$ is found by performing a linear regression of $\ln \sum_{i=1}^{N_l} p_i^q(l)$ with $\ln \delta$ in a finite interval of δ (usually $a/L \leq \delta \leq 1/2$). In order to properly satisfy the previous conditions (5) and (4), in this work we will compute the derivative

$$\tau_q(L) = \left. \frac{d \ln \sum_{i=1}^{N_l} p_i^q(l)}{d \ln \delta} \right|_{\delta=0.1}. \quad (6)$$

First, $\tau_q(L)$ was calculated for different system sizes and then extrapolated to the macroscopic limit, $\tau_q = \lim_{L \rightarrow \infty} \tau_q(L)$.

III. RESULTS

A. Weak coupling regime ($b \gg 1$)

Using the exact eigenstates of Hamiltonian (2) obtained from numerical diagonalizations, we evaluate, for each value of q , L and b , the numerator on the right-hand side of Eq. (4) for decreasing box sizes, and then calculate $\tau_q(L)$ from the slope of the graph of the numerator versus $\ln \delta$ at $\delta = 0.1$, Eq. (6). Fig. 1 provides an example of the $\ln \delta$ dependence of $\ln \sum_{i=1}^{N_l} p_i^q(l)$ in the weak coupling regime ($b = 10$) for a system size $L = 5400$ and different values of q : 4 (circles), 5 (triangles), 6 (diamonds)

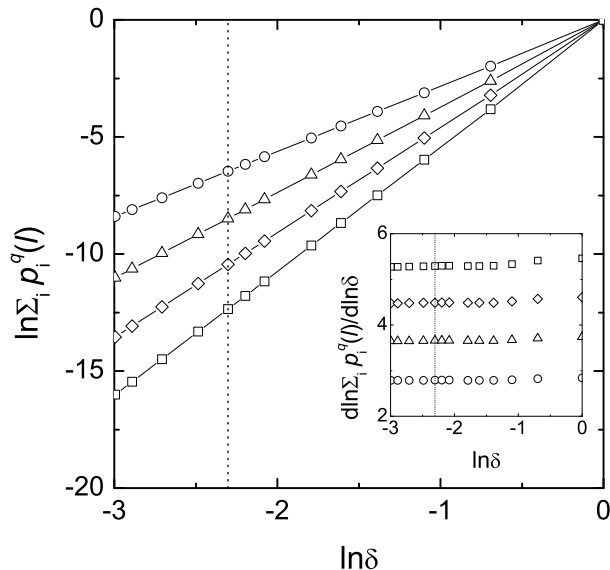


FIG. 1: The $\ln \delta$ dependence of $\ln \sum_{i=1}^{N_l} p_i^q(l)$ in the weak coupling regime ($b = 10$) for $L = 5400$ and different q values: $q = 4$ (circles), 5 (triangles), 6 (diamonds) and 7 (squares); the dotted vertical line corresponds to $\delta = 0.1$. The inset shows the same dependence of corresponding slopes, $d \ln \sum_{i=1}^{N_l} p_i^q(l) / d \ln \delta$.

and 7 (squares); the dotted vertical line corresponds to $\delta = 0.1$. The inset shows the same dependence of the corresponding slopes, $d \ln \sum_{i=1}^{N_l} p_i^q(l) / d \ln \delta$. Note that these derivatives are practically constant in the region shown. We have checked that the results are practically the same when $\tau_q(L)$ was obtained from the linear fit to $\ln \sum_{i=1}^{N_l} p_i^q(l)$ vs $\ln \delta$ in the interval $0.1 \lesssim \delta \lesssim 0.4$.

The size dependence of $\tau_q(L)$ at the critical point of the finite system for $b = 10$ is shown in Fig. 2 for $q = 4$. Clearly, significant finite size effects are present and for the larger values of L the convergence is evident. In order to predict the asymptotic value of τ_q from such a plot, a curve of the form $\tau_q(L) = \tau_q + F_{a_q, c_q}(L)$ was fitted to the data points in this graph, where τ_q , a_q and c_q are three fitting parameters and $F_{a_q, c_q}(L)$ is a function which tends to zero as $L \rightarrow \infty$. Various forms for $F_{a_q, c_q}(L)$ were chosen and tested on the data plots, including exponential ($\sim e^{-c_q L}$), inverse logarithmic ($\sim 1 / \ln c_q L$) and power law ($\sim L^{-c_q}$) decay with L . The testing involved performing a three parameter fit on the $\tau_q(L)$ vs L data plots using the standard Levenberg-Marquardt method for non-linear fits. The form of $F_{a_q, c_q}(L)$ eventually chosen was the power law. The reason for choosing the above form with preference to the alternative forms was simply that the inverse logarithmic and the exponential laws did not fit our data properly. In addition, for all values of q and b we found that the exponent c_q hardly differs from unity. Thus, we can write

$$\tau_q(L) = \tau_q + a_q/L, \quad (7)$$

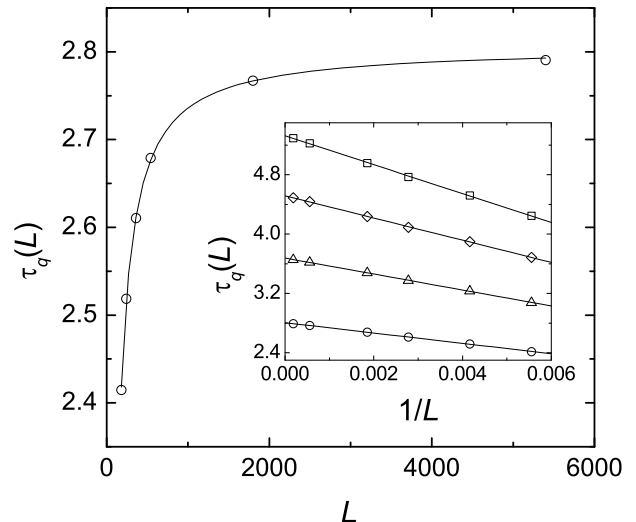


FIG. 2: The L dependence of the mass exponent $\tau_q(L)$ in the weak coupling regime ($b = 10$) for $q = 4$ (circles); solid line is a fit to Eq. (7). The inset shows $\tau_q(L)$ on a $1/L$ scale for different q values: $q = 4$ (circles), 5 (triangles), 6 (diamonds) and 7 (squares); the straight lines are linear fits to Eq. (7).

and keep only two free parameters. The solid line in Fig. 2 is a fit to Eq. (7). Note that this equation gives a fairly good fit to the data. $\tau_q(L)$ is represented on a $1/L$ scale in the inset of Fig. 2 for different values of q : 4 (circles), 5 (triangles), 6 (diamonds) and 7 (squares). Here, one can better appreciate the linear behavior, Eq. (7), of the finite size corrections to τ_q .

The q -dependence of the extrapolated results of $d_q = \tau_q / (q - 1)$ in the weak coupling regime are depicted in the inset of Fig. 3 for several values of b : 6 (squares), 8 (triangles), 10 (diamonds) and 12 (circles). The solid lines are fits to the form $d_q = 1 - c_b q$. The corresponding b -dependent slopes, c_b , are summarized and compared with the nonlinear σ -model estimates, $1/2\pi b$, in Fig. 5. The main panel shows the same data d_q as a function of the rescaled variable $q/2\pi b$, in which it is clearly seen that the data points collapse fairly well onto a single straight line according to Eq. (3) (solid line). To our knowledge, this result provides the first numerical test of the nonlinear σ -model prediction for the PRBM model.

B. Strong coupling regime ($b \ll 1$)

We have also calculated d_q for the critical wavefunctions of Hamiltonian (2) in the strong coupling regime for which, as we already mentioned, there is no analytical predictions for values of $q \lesssim b \ll 1$. The only analytical estimate in this regime was obtained for $q > 1/2$, based on a resonance pairs approximation, in Ref.¹⁸. The $\tau_q \simeq 4b\Gamma(q - \frac{1}{2})/\sqrt{\pi}\Gamma(q - 1)$ found diverges at $q = 1/2$ and for smaller values of q this approximation completely

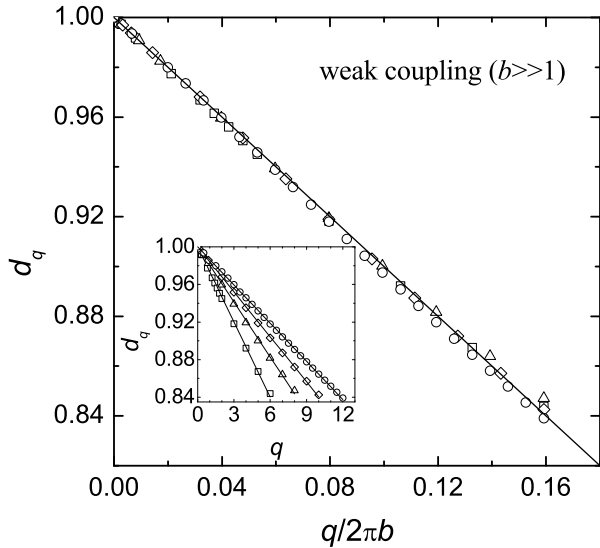


FIG. 3: d_q as a function of the rescaled variable $q/2\pi b$ in the weak coupling regime ($b \gg 1$) for several b values: 6 (squares), 8 (triangles), 10 (diamonds) and 12 (circles); the solid line represents the nonlinear σ -model estimate, Eq. (3). The inset shows the same data on the scale q ; solid lines are fits to the form $d_q = 1 - c_b q$.

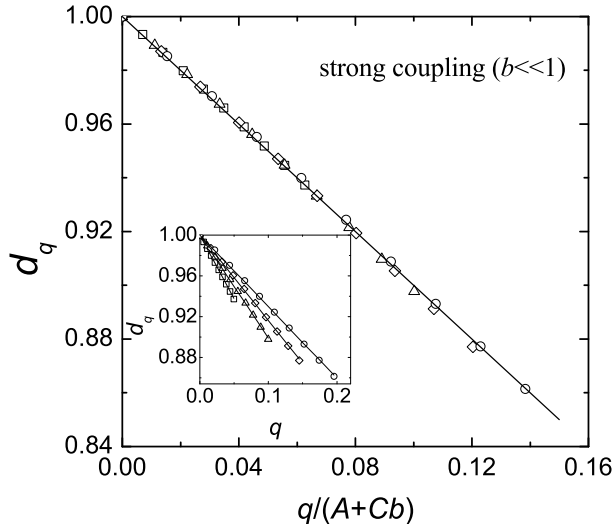


FIG. 4: As for Fig. 3, for the strong coupling regime ($b \ll 1$): $b = 0.05$ (squares), 0.1 (triangles), 0.15 (diamonds) and 0.2 (circles). The solid line corresponds to Eq. (8). The straight lines in the inset are fits to the form $d_q = 1 - c_b q$.

breaks down.

Figure 4 shows the same extrapolated values of d_q as for Fig. 3 in the strong coupling regime ($b \ll 1$). The values of b reported are 0.05 (squares), 0.1 (triangles), 0.15 (diamonds) and 0.2 (circles), and the corresponding slopes c_b are summarized in Fig. 5 (solid circles). As in

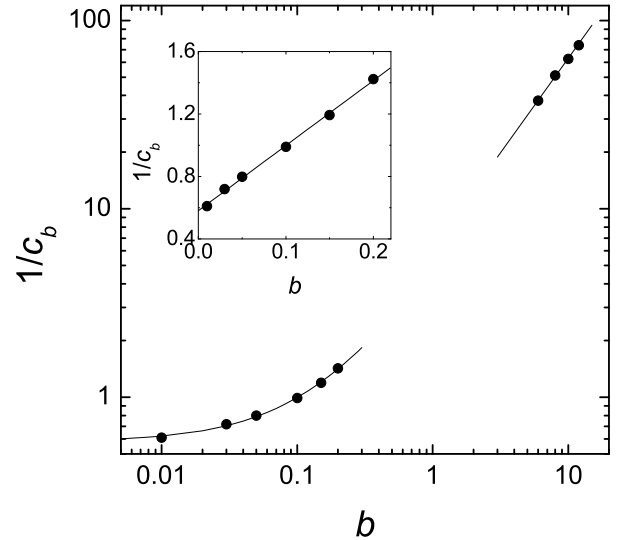


FIG. 5: The inverse slope $1/c_b$ (solid circles) of the fractal dimension as a function of the parameter b of the PRBM model. The solid lines represent the analytical asymptotic ($b \gg 1$) result, $2\pi b$, and the strong coupling ($b \ll 1$) result proposed in this work, $A + Cb$. The small- b behavior of $1/c_b$ is reported in the inset; the straight line is a linear fit to the form $A + Cb$.

the weak disorder case, a linear dependence of d_q on q is found for $q \lesssim b$. In order to collapse all data points onto a single straight line, as was done for the opposite limit $b \gg 1$, we propose the relation $1/c_b = A + Cb$ for the slopes, where $A \neq 0$ and C are two fitting parameters (see inset of Fig. 5). The collapse of the data is evident from the main panel of Fig. 4, when these data are represented as a function of the rescaled variable $q/(A + Cb)$. Hence, the q -dependence of d_q in the limit $b \ll 1$ can be described by the linear relation

$$d_q = 1 - \frac{q}{A + Cb}, \quad q \lesssim b. \quad (8)$$

This equation constitutes the main result of the present publication. Thus, our results suggest the intriguing possibility that the linear dependence of d_q on q seems to be a generic law valid in all regimes. Although this is a conjecture at the present state, we expect that it will stimulate further analytical work.

The inverse slope $1/c_b$ of d_q is depicted on a log-log plot in Fig. 5 (solid circles) as a function of parameter b of the PRBM model. The inset shows the small- b dependence of $1/c_b$, from which the linear behavior on b is evident; the straight line is a linear fit to the proposed form with parameters $A = 0.580 \pm 0.009$ and $C = 4.17 \pm 0.08$. The numerical calculations agree perfectly with the analytical asymptotic in the weak coupling regime $b \gg 1$, $1/c_b = 2\pi b$, and with the form proposed of this work for the strong coupling regime $b \ll 1$, $1/c_b = 0.58 + 4.17b$.

IV. SUMMARY

In this paper we have calculated the fractal dimensions d_q of the wavefunctions for 1D disordered systems with long-range transfer terms at criticality. The leading finite-size corrections to d_q decay algebraically with exponents equal to minus one. At the infinite-size limit, we have confirmed that, according to theoretical predictions, d_q is linearly dependent on q in the weak coupling regime. Our calculations strongly suggest that this behavior is also valid at strong coupling. So, the linear dependence of d_q on q seems to be a generic law valid in all disorder regimes.

The question arises as to whether these results are applicable to other quantum systems, particularly in the 3D Anderson transition that occurs in the strong disorder domain, and whose similarity with the PRBM model at $b = 0.3$ has been demonstrated for several critical magnitudes⁵.

Acknowledgments

We would like to thank the Spanish DGESIC for financial support through project number BFM2000-1059.

-
- * Electronic address: ecr@um.es;
URL: <http://bohr.fcu.um.es/miembros/ecr/>
- ¹ H.G.E. Hentschel and I. Procaccia, *Physica D* **8**, 435 (1983).
 - ² M. Janssen, *Int. J. Mod. Phys. B* **8**, 943 (1994); B. Huckestein, *Rev. Mod. Phys.* **67**, 357 (1995).
 - ³ V.I. Falko and K.B. Efetov, *Europhys. Lett.* **32**, 627 (1995); *Phys. Rev. B* **52**, 17413 (1995).
 - ⁴ A.D. Mirlin, *Phys. Rep.* **326**, 259 (2000); F. Evers and A.D. Mirlin, *Phys. Rev. Lett.* **84**, 3690 (2000).
 - ⁵ E. Cuevas, M. Ortuño, V. Gasparian, and A. Pérez-Garrido, *Phys. Rev. Lett.* **88**, 016401 (2002).
 - ⁶ K.B. Efetov, *Adv. Phys.* **32**, 53 (1983).
 - ⁷ F. Wegner, *Z. Phys. B* **36**, 209 (1980); C. Castellani and L. Peliti, *J. Phys. A: Math. Gen.* **19**, L429 (1986); B.L. Altshuler, V.E. Kravtsov and I.V. Lerner, *Zh. Eksp. Teor. Fiz.* **91**, 2276 (1986) [*Sov. Phys. JETP* **64**, 1352 (1986)].
 - ⁸ A.D. Mirlin, Y.V. Fyodorov, F.M. Dittes, J. Quezada and T.H. Seligman, *Phys. Rev. E* **54**, 3221 (1996).
 - ⁹ Andreas W. W. Ludwig, Matthew P. A. Fisher, R. Shankar and G. Grinstein, *Phys. Rev. B* **50**, 7526 (1994).
 - ¹⁰ C.C. Chamon, C. Mudry, and X.-G. Wen, *Phys. Rev. Lett.* **77**, 4194 (1996); H.E. Castillo, C.C. Chamon, E. Fradkin, P.M. Goldbart, and C. Mudry, *Phys. Rev. B* **56**, 10668 (1997).
 - ¹¹ David Carpentier and Pierre Le Doussal, *Phys. Rev. E* **63**, 026110 (2001).
 - ¹² M.J. Bhaseen, I.I. Kogan, O.A. Soloviev, N. Taniguchi, and A.M. Tsvelik, *Nucl. Phys. B* **580**, 688 (2000).
 - ¹³ D. A. Parshin and H. R. Schober, *Phys. Rev. B* **57**, 10232 (1998).
 - ¹⁴ H. Potempa and L. Schweitzer, *Phys. Rev. B* **65**, 201105(R) (2002).
 - ¹⁵ P.W. Anderson, *Phys. Rev.* **109**, 1492 (1958).
 - ¹⁶ L.S. Levitov, *Europhys. Lett.* **9**, 83 (1989); *Phys. Rev. Lett.* **64**, 547 (1990).
 - ¹⁷ L.S. Levitov, *Ann. Phys. (Leipzig)* **8**, 697 (1999).
 - ¹⁸ A.D. Mirlin and F. Evers, *Phys. Rev. B* **62**, 7920 (2000).
 - ¹⁹ E. Cuevas, V. Gasparian and M. Ortuño, *Phys. Rev. Lett.* **87**, 056601 (2001); E. Cuevas, *Phys. Rev. B* **66**, 233103 (2002).
 - ²⁰ I. Varga and D. Braun, *Phys. Rev. B* **61**, R11859 (2000); Imre Varga, *Phys. Rev. B* **66**, 094201 (2002).
 - ²¹ E. Cuevas, cond-mat/0209618.
 - ²² V.E. Kravtsov and K.A. Muttalib, *Phys. Rev. Lett.* **79**, 1913 (1997).
 - ²³ V.E. Kravtsov and A.M. Tsvelik, *Phys. Rev. B* **62**, 9888 (2000).
 - ²⁴ E. Cuevas, *Phys. Rev. Lett.* **83**, 140 (1999); E. Cuevas, E. Louis, and J.A. Vergés, *Phys. Rev. Lett.* **77**, 1970 (1996).
 - ²⁵ Ashvin Chhabra and Roderick V. Jensen, *Phys. Rev. Lett.* **62**, 1327 (1989).